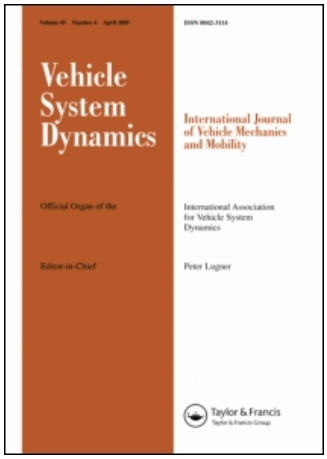

Vehicle System Dynamics
International Journal of Vehicle Mechanics and Mobility
Publication details, including instructions for authors and subscription information:
http://www.informaworld.com/smpp/title~content=t713659010

Practical vehicle rollover avoidance control using energy method

Seibum B. Choi [a]
[a] Graduate School of Automobile Technology, Korea Advanced Institute of Science and Technology, Daejeon, South Korea

Online Publication Date: 01 April 2008
To cite this Article: Choi, Seibum B. (2008) 'Practical vehicle rollover avoidance control using energy method', Vehicle System Dynamics, 46:4, 323 - 337
To link to this article: DOI: 10.1080/00423110701377109
URL: http://dx.doi.org/10.1080/00423110701377109

Vehicle System Dynamics
Vol. 46, No. 4, April 2008, 323–337

Taylor & Francis
Taylor & Francis Group

Practical vehicle rollover avoidance control using energy method

SEIBUM B. CHOI*

Graduate School of Automobile Technology, Korea Advanced Institute of Science and Technology, Science Town, Daejeon 305-701, South Korea

In this paper, a novel rollover prevention control algorithm is developed for application on vehicles with a high centre of gravity. The developed algorithm can be implemented on any vehicle equipped with an electronic stability program with or without an extra roll rate sensor. The vehicle rollover index is defined from the vehicle lateral kinetic energy and the new concept of virtual gravity. The algorithm is implemented on a production hydraulic control unit and tested using a typical medium size sport utility vehicle up to a speed of 110 km h^{-1}. The test results show that the control algorithm prevents the vehicle rollover very successfully without any noticeable false activation or over correction resulting in severe under steer. Also, the controlled wheel speed shows a very stable and smooth trace.

Keywords: Rollover; Control; Energy; Vehicle

Nomenclature

a	distance from vehicle C.G. to front axle, m
A_{Th}	rollover index acceleration threshold, unitless
a_{ym}	measured vehicle lateral acceleration, m s^{-2}
a_{yMod}	lead compensated vehicle lateral acceleration, m s^{-2}
b	distance from vehicle C.G. to rear axle, m
C.G.	centre of gravity
c_t	suspension roll damping coefficient, N-m*(rad s^{-1})$^{-1}$
d	one half of vehicle track width, m
$\mathrm{ESPP}_{\mathrm{cmd}}$	pressure control command from ESP, bar
Fz	tire normal load, N
g	gravity constant, m s^{-2}
h	nominal C.G. height, m
I_x	vehicle angular momentum with respect to x-axis, kg-m^2
k_a	C.G. height adaptation gain of roll dynamics observer, unitless positive constant
k_o	roll rate error gain of roll dynamics observer, unitless positive constant
k_t	suspension roll spring coefficient, N-m rad^{-1}
LF	left front wheel

*Email: sbchoi@kaist.ac.kr

Vehicle System Dynamics
ISSN 0042-3114 print/ISSN 1744-5159 online © 2008 Taylor & Francis
http://www.informaworld.com
DOI: 10.1080/00423110701377109

M	vehicle mass, kg
P_{bm}	measured wheel pressure, bar
P_{cmd}	wheel pressure control command, bar
RF	right front wheel
RSCP_{cmd}	pressure control command from rollover avoidance controller, bar
S_{cmd}	wheel slip control command, m s^{-1}
SGR	steering wheel gear ratio, unitless constant
SWA	steering wheel angle, radian
V_{ch}	characteristic speed, m s^{-1}
V_w	wheel speed, m s^{-1}
V_x	vehicle longitudinal velocity, m s^{-1}
V_y	vehicle lateral velocity, m s^{-1}
x, y	sprung mass coordinates
x', y'	virtual gravity coordinates
yaw	vehicle yaw rate, rad s^{-1}
β	vehicle side slip angle, radian
β Mod	lead compensated vehicle side slip angle, radian
λ	constant associated with roll dynamics observer, unitless
μ	road-to-tire friction coefficient, unitless
σ	tangent angle representing force ratio, radian
φ	roll angle of vehicle sprung mass, radian
Φ	rollover index, $(\text{m s}^{-1})^2$
Φ_0	rollover potentiality index, $(\text{m s}^{-1})^2$

1. Introduction

Contrary to common opinion, sport utility vehicles (SUV) are not safer than passenger cars in fatal accidents. This is due to the high rollover propensity of SUV and the high fatality rate associated with the rollover accident. Statistically, the fatality rate for accidents involving the rollover of SUV is as high as 59% [1]. The vehicle stability control systems can reduce the chance of vehicle rollover induced by the over steering condition [2, 3]. However, this condition is not always the cause of the rollover even for the non-tripped rollover cases. For example, vehicles can be neutrally or under steered but can still have a large side slip angle that is interpreted as the large amount of lateral kinetic energy. The lateral kinetic energy can be converted to roll kinetic energy very quickly. Also, the vehicle rollover is significantly affected by the suspension design, especially the dampers as well as the driving conditions. Therefore, a vehicle can be rolled over for lateral acceleration that is far less than the statically critical one. Usually, the yaw stability of a vehicle, and therefore the performance of the electronic stability program (ESP), is much less affected by the damper characteristics.

There have been many efforts to prevent the rollover. However, most of the solutions are found to be too expensive due to the cost of the extra sensors and/or actuators, or too slow to prevent the rollover, especially for the very dynamic fishhook type maneuvers [4–10]. Considering quick roll dynamics and the slow brake response of the high C.G. SUV/truck type vehicles, it is very critical to activate the brake control very early, at the moment when the rollover is far from being imminent. At the same time, any false activation that can be noticed by the driver must be prevented.

In this paper, a very practical rollover avoidance control algorithm is developed which can be implemented with no or very little extra cost on a vehicle equipped with ESP. The vehicle rollover is prevented by the brake control only. The roll rate sensor can be added optionally

to enhance the performance or minimize false activation. The algorithm is developed for application on high C.G. vehicles with a slow brake actuator like SUVs and light trucks. However, the same algorithm can be applied to any other types of vehicles with no technical difficulty or extra cost.

Most of the existing rollover prevention controls estimate the rollover propensity by measuring or estimating the vehicle roll angle and/or roll rate. These controls are most effective only for slow and less dynamic situations like J-turn maneuver, and the extra cost for the sensing is an issue. In this paper, an indirect rollover estimation method is suggested. The suggested method predicts the propensity of vehicle rollover by monitoring the lateral kinetic energy and the lateral acceleration of a vehicle. The lateral kinetic energy is calculated through the vehicle longitudinal velocity and the vehicle side slip angle, which is estimated using yaw stability control sensors and vehicle dynamic model. This method predicts the rollover propensity fairly accurately without a roll angle or a roll rate sensor. It is also a very effective way to estimate the rollover propensity with enough lead time. Considering the slow brake response time of the light trucks and the very dynamic nature of a fishhook type maneuver, the control effort needs to be initiated very early with enough lead time when the vehicle roll angle and/or roll rate is not significant. Frequently, this type of maneuver leads to the most severe rollover accident. However, the developed rollover avoidance controller can prevent the fatal rollover in a very cost efficient way.

Figure 1 shows the roll dynamic response of a typical mid-size SUV for fishhook type steering input. The rollover prevention control is not active and the vehicle speed is 100 km h^{-1}. When the roll angle reaches 90°, the vehicle is declared to be rolled over. However, for the roll angle of as little as 10–15°, the inside wheels are lifted from the ground, and the brake control to prevent the rollover becomes useless. The transition time from 0° roll angle to 10° degrees is less than one-half second, while the combined delay and lag of the brake actuator is more than that. One-half second prior to the point of the wheel lift, both the roll angle and the roll dynamic energy are very small, and the vehicle shows no sign of rollover. Therefore, it is

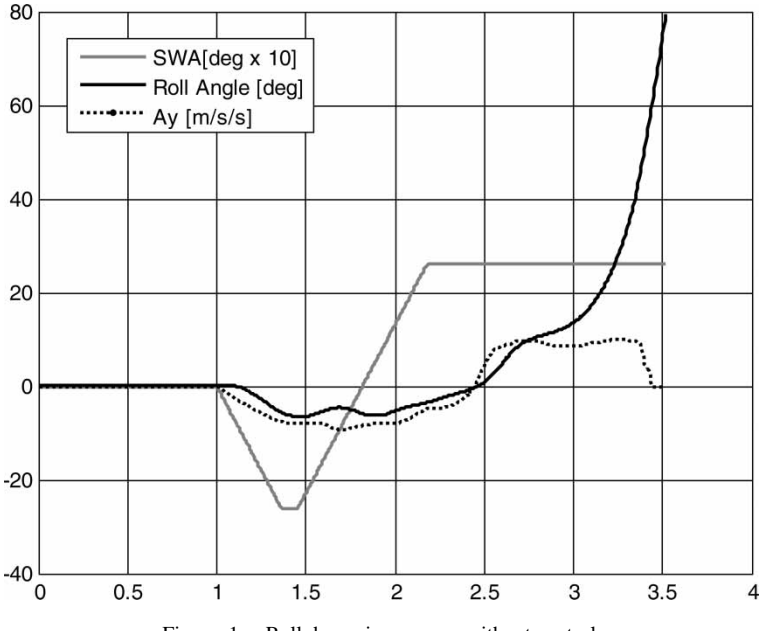

Figure 1. Roll dynamic response without control.

necessary to monitor the vehicle response beyond the roll angle or roll rate to prevent rollover for driving situations with a very dynamic steering input.

2. Rollover estimation algorithm

There have been several efforts to predict vehicle rollover using the vehicle roll energy and the tipover potential energy [11]. These efforts are effective to monitor the process of vehicle rollover, but tend to be too slow to actively prevent the rollover, especially for high C.G. vehicles with slow brake actuators. In this section, rollover index (ROI) is defined from the vehicle lateral kinetic energy and the virtual gravity. ROI represents the rollover propensity of the vehicle. Figure 2 shows the diagram of the front view of a vehicle sprung mass where y and z axes are fixed to the sprung mass C.G. and rotate with the mass. a_{ym} is the lateral acceleration measured by the accelerometer attached to the vehicle sprung mass. The measured acceleration is partly from the vehicle acceleration and partly from gravity. φ is the absolute roll angle of the vehicle sprung mass with respect to the earth coordinates due to the lateral acceleration and/or the super elevation angle of the road surface.

If the artificial angle σ is defined by the tangent ratio of a_{ym} and $g\cos(\varphi)$ as follows:

$$\tan\sigma \equiv \frac{a_{ym}}{g\cos\varphi} \tag{1}$$

then, figure 2 can be reconfigured as figure 3.

In the reconfigured coordinates, z' axis is defined as parallel to the direction of the net force on the vehicle sprung mass. Defining the net acceleration $g\cos(\varphi)/\cos(\sigma)$ on the vehicle mass as virtual gravity, the problem can be equated to a mass on a σ degree hill with a gravity constant of $g\cos(\varphi)/\cos(\sigma)$.

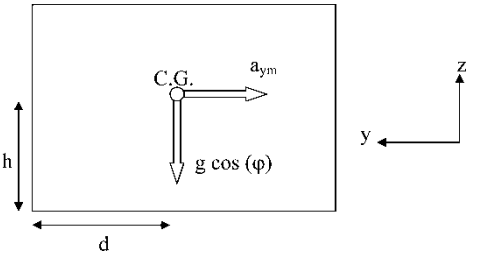

Figure 2. Diagram of vehicle coordinates.

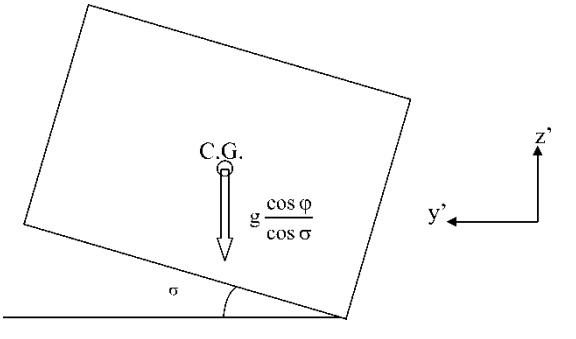

Figure 3. Diagram of a vehicle in virtual gravity coordinates.

In figure 2, the current height of C.G. is $d\sin(\sigma) + h\cos(\sigma)$, and the critical height of C.G., where the vehicle is at the verge of rollover, is $\sqrt{d^2 + h^2}$. Therefore, defining the height change of C.G. required for rollover as Δh:

$$\begin{aligned}\Delta h &= \sqrt{d^2 + h^2} - (d\sin\sigma + h\cos\sigma) \\ &= \sqrt{d^2 + h^2} - \frac{da_{\text{ym}} + hg\cos\varphi}{\sqrt{g^2\cos^2\varphi + a_{\text{ym}}^2}}\end{aligned} \tag{2}$$

The minimum amount of potential energy – normalized with the vehicle mass – required for the rollover is defined as $(g\cos\varphi/\cos\sigma)^*\Delta h$ using the concept of virtual gravity constant. Since the lateral kinetic energy of a vehicle can be converted to potential energy very quickly through the roll motion, a vehicle has the potential to rollover as long as the lateral energy is larger or equal to the minimum required potential energy, i.e.:

$$\begin{aligned}\frac{1}{2}V_y^2 > \frac{g\cos\varphi}{\cos\sigma}\Delta h &= \sqrt{g^2\cos^2\varphi + a_{\text{ym}}^2}\,\Delta h \\ &= \sqrt{g^2\cos^2\varphi + a_{\text{ym}}^2}\sqrt{d^2 + h^2} - (da_{\text{ym}} + hg\cos\varphi)\end{aligned} \tag{3}$$

The lateral velocity V_y can be calculated from longitudinal velocity V_x and vehicle side slip angle β as:

$$V_y = V_x\beta \tag{4}$$

V_x is calculated from the measured wheel speeds. Usually, β can not be measured directly using a sensor at a commercially reasonable cost. However, several methods have been developed to estimate β from the measured yaw rate, lateral acceleration, steering wheel angle and vehicle dynamic model like the bicycle model [12–16]. The accuracy of the estimation can be further enhanced with the additional multi-axis G sensor information [17]. There exist other approaches to estimate β from the indirect measurement of the tire forces [18]. Further detail of the β estimation algorithm is beyond the scope of this paper. In general, the current production ESP algorithms have some problems in providing accurate estimation of the side slip angle, especially during the long-term maneuvers with excessive side slip or on a severe bank. However, the estimation is known to be quite accurate during the quick dynamic maneuvers especially on a flat surface. Since the application of the rollover prevention control is limited only to the cases of very quick and dynamic fishhook type maneuvers completed in a short time period, the estimation from the production ESP algorithm is acceptable for the purpose of the rollover control.

Motivated by the above inequality condition, a rollover potentiality index Φ_0 is defined as follows:

$$\Phi_0 = \frac{1}{2}|V_x\beta|^2 - \sqrt{g^2 + a_{\text{ym}}^2}\sqrt{d^2 + h^2} + da_{\text{ym}} + hg \tag{5}$$

While defining Φ_0 from the above inequality condition, $\cos\varphi$ is neglected. Rollover detection algorithm is required to detect rollover before the roll angle becomes excessive. Even when the angle φ is as large as 25°, $\cos\varphi$ is 0.9, and the effect of neglecting $\cos\varphi$ on defining Φ_0 is less than 0.4% of Φ_0 itself. Since this error is much less than the other uncertainties of the vehicle parameters and the estimated vehicle side slip angle, it can be claimed that the effect of the roll angle φ on defining Φ_0 is negligible. Practically, it is required to detect the rollover when the roll angle is far less than 8° or so.

Positive Φ_0 means that the vehicle has the potential to rollover, and the possibility of rollover increases with Φ_0. Large Φ_0 alone does not mean the vehicle will rollover. The large kinetic

energy needs to be converted to roll dynamic energy. It usually happens when a vehicle hits a high μ surface or a bump after a large side slip typically on a low μ surface. If the vehicle hits a high μ surface, the lateral acceleration of the vehicle increases very quickly. In this paper, it is determined after the analysis of the simulation results that the measured lateral acceleration needs to be more than 80% of statically critical lateral acceleration for rollover to happen. However, this 80% acceleration threshold (A_{Th}) needs to be tuned for different vehicles with different vehicle parameters and suspension characteristics. Statically, critical lateral acceleration is defined as the acceleration to make a vehicle to rollover statically on a flat surface and described as $(d/h) * g$.

Of Φ_0 and measured lateral acceleration, ROI is defined as follows:

$$\Phi = \Phi_0 \times \left(|a_{\mathrm{ym}}| - \frac{d}{h} g \times A_{\mathrm{Th}} > 0 \right) \tag{6}$$

The ROI is rollover potentiality index switched on or off determined by the magnitude of the measured acceleration. If the absolute value of the measured lateral acceleration is less then the statically critical acceleration weighted by the threshold A_{Th}, the index is zero. The threshold of the index itself to trigger roll stability control is yet to be fine tuned by field tests, considering the uncertainties of the vehicle parameters and the estimated vehicle side slip angle as well as the vehicle suspension dynamics. It should be noted that the defined ROI is the extension and the generalization of the statically critical lateral acceleration to initiate the vehicle rollover. Assuming that a vehicle is simplified as a rectangular box and the road surface friction is large enough, then the statically critical lateral acceleration is equal to $g * (d/h)$. Equation (5) shows that the index is equal to zero when the side slip angle is zero and the lateral acceleration is $g * (d/h)$. Under the existence of the side slip angle, the index becomes equal to zero for the lateral acceleration that is less than the statically critical one.

3. Vehicle parameter estimation

In the previous section, ROI is defined just as a function of the lateral kinetic energy and the potential energy. That definition is fine for most of the dynamic rollover cases. However, there is an advantage of considering the roll kinetic energy for the slow rollover cases. It is also helpful to update the C.G. height information dynamically [19, 20]. In this section, the vehicle roll angle and the C.G. height are estimated from the measured roll rate and the vehicle dynamic model. The estimated C.G. height information can be used to enhance the accuracy of ROI.

The simplified linear second order roll dynamics of a vehicle is described as follows:

$$I_x \ddot{\theta} = M a_{\mathrm{ym}} h - k_t \theta - c_t \dot{\theta} \tag{7}$$

where the bouncing motion of the sprung mass is neglected. Also, this simplified dynamic model is valid only to the point where the inside wheels are lifted from the ground. The static balance of the forces, and therefore the gravity force, is excluded from the above equation. Motivated by the roll dynamics equation (7), a roll dynamics observer is defined using the measured roll rate $\dot{\theta}$ and the estimated C.G. height $\hat{h}$ as follows:

$$I_x \ddot{\hat{\theta}} = M a_{\mathrm{ym}} \hat{h} - k_t \hat{\theta} - c_t \dot{\hat{\theta}} + k_0 (\dot{\theta} - \dot{\hat{\theta}}) \tag{8}$$

Defining the estimation errors of the roll angle and the C.G. height as follows:

$$\tilde{\theta} \equiv \theta - \hat{\theta} \tag{9}$$

$$\tilde{h} \equiv h - \hat{h} \tag{10}$$

and, subtracting equation (8) from equation (7), the error dynamics of the observer is described as follows:

$$I_x\ddot{\tilde{\theta}} = Ma_{\mathrm{ym}}\tilde{h} - k_t\tilde{\theta} - c_t\dot{\tilde{\theta}} - k_0\dot{\tilde{\theta}} \tag{11}$$

or, equivalently as:

$$I_x\ddot{\tilde{\theta}} + (c_t + k_0)\dot{\tilde{\theta}} + k_t\tilde{\theta} = Ma_{\mathrm{ym}}\tilde{h} \tag{12}$$

The stability of the roll dynamics observer is evaluated through Lyapunov stability analysis. Also the C.G. height adaptation algorithm is derived through the same analysis. Let a positive definite scalar function V be defined as follows:

$$V \equiv \frac{1}{2}(\dot{\tilde{\theta}} + \lambda\tilde{\theta})^2 + \frac{1}{2}\frac{1}{k_a}\tilde{h}^2 > 0 \tag{13}$$

where λ is a constant that is yet to be determined.

Differentiating equation (13) and combining it with the differentiation of equation (10):

$$\dot{V} = (\dot{\tilde{\theta}} + \lambda\tilde{\theta})(\ddot{\tilde{\theta}} + \lambda\dot{\tilde{\theta}}) - \frac{1}{k_a}\tilde{h}\dot{\tilde{h}} \tag{14}$$

Combining equations (11) and (14):

$$\begin{aligned}\dot{V} &= (\dot{\tilde{\theta}} + \lambda\tilde{\theta})\left(-\frac{c_t + k_0 - I_x\lambda}{I_x}\dot{\tilde{\theta}} - \frac{k_t}{I_x}\tilde{\theta}\right) + \left[\frac{M}{I_x}(\dot{\tilde{\theta}} + \lambda\tilde{\theta})a_{\mathrm{ym}} - \frac{1}{k_a}\dot{\tilde{h}}\right]\tilde{h} \\ &= -\frac{c_t + k_0 - I_x\lambda}{I_x}(\dot{\tilde{\theta}} + \lambda\tilde{\theta})\left(\dot{\tilde{\theta}} + \frac{k_t}{c_t + k_0 - I_x\lambda}\tilde{\theta}\right) + \left[\frac{M}{I_x}(\dot{\tilde{\theta}} + \lambda\tilde{\theta})a_{\mathrm{ym}} - \frac{1}{k_a}\dot{\tilde{h}}\right]\tilde{h}\end{aligned} \tag{15}$$

Define λ such that:

$$\lambda = \frac{k_t}{c_t + k_0 - I_x\lambda} \tag{16}$$

i.e.

$$\lambda = \frac{c_t + k_0 \pm \sqrt{(c_t + k_0)^2 - 4I_xk_t}}{2I_x} \tag{17}$$

then,

$$\dot{V} = -\frac{c_t + k_0 - I_x\lambda}{\mathrm{I}_x}(\dot{\tilde{\theta}} + \lambda\tilde{\theta})^2 + \left[\frac{M}{I_x}(\dot{\tilde{\theta}} + \lambda\tilde{\theta})a_{\mathrm{ym}} - \frac{1}{k_a}\dot{\tilde{h}}\right]\tilde{h} \tag{18}$$

Now update $\hat{h}$ such that:

$$\dot{\hat{h}} = \frac{k_aM}{I_x}(\dot{\tilde{\theta}} + \lambda\tilde{\theta})a_{\mathrm{ym}} \tag{19}$$

then, equation (18) can be written as follows:

$$\dot{V} = -\frac{c_t + k_0 - I_x\lambda}{I_x}(\dot{\tilde{\theta}} + \lambda\tilde{\theta})^2 \tag{20}$$

Equation (20) shows that, $\dot{V}$ is negative semi-definite for the positive constant observer gain k_0 greater than $(I_x\lambda - c_t)$. Therefore, the error of the roll angle estimation converges to zero

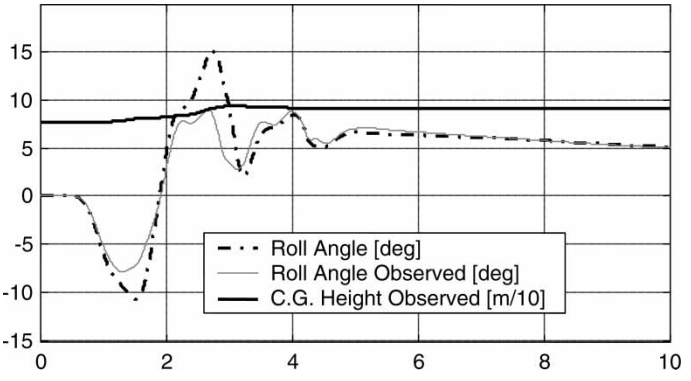

Figure 4. Roll dynamics observer with parameter estimation.

under the condition of the persistent actuation. Also, the error dynamics equation (12) shows that the C.G. height estimation error converges to zero too.

The developed roll dynamics observer is implemented on Simulink and simulated with the model of a mid-size SUV from GM. For the vehicle simulation, CarSim commercial vehicle simulation software is used. The software allows the link to Simulink that provides the observer output. The used vehicle model parameters and the observer gains are: $I_x = 1{,}195$ kg-m^2, $M = 2333$ kg, $h = 0.762$ m, $k_t = 143{,}000$ N-m rad^{-1}, $c_t = 14{,}800$ N-m $*$ (rad sec^{-1})$^{-1}$, $k_o = 11{,}345$, and $k_a = 0.01$.

Figure 4 shows the simulation result of the closed loop observer for a fishhook type steering maneuver. The driver throttle and brake inputs are set to zero, and the roll avoidance control is active. The vehicle has 100 kg of load at the roof top. The load increases the C.G. height of the gross vehicle by around 10%, and the height observer is tracking the increased height fairly well. Correspondingly, the observed roll angle is converging to the true value. At the extreme roll angles, the observer shows some tracking error. That is mostly due to the non-linearity of the vehicle suspension system. The transient response of the observer during the extreme events can be improved by refining the vehicle suspension model or simply by increasing the observer gain – it depends upon the accuracy of the roll rate sensor. Since the purpose of implementing the roll dynamics observer is in activating the rollover avoidance control far before the roll angle reaches the critical rollover point, the accuracy of the observer beyond 5–7° roll angle might be meaningless.

4. Lead compensation of measured signals

As mentioned previously, the brake response of the light truck is slow while the roll dynamics is very fast due to the nature of the high C.G. vehicles. The signals used to define ROI – lateral acceleration and vehicle side slip angle – need to be lead compensated to cancel the lag effect of the brake actuation. As figure 5 shows, the steering wheel angle signal precedes all the other vehicle dynamic signals significantly and is also very clean. Therefore, it makes sense to have the measured signals lead compensated using the steering wheel angle signal and the vehicle lateral dynamic model.

The bicycle model of a vehicle is widely used to express the lateral dynamics of a vehicle as a function of steering wheel input [21]. This model assumes that the left and the right wheels are put at the same central locations along the vehicle centre line (x-axis). At the steady state,

the bicycle model can be further simplified as follows:

$$a_y = \frac{V_x^2}{(a+b)[1+(V_x/V_{\text{ch}})^2]}\left(\frac{\text{SWA}}{\text{SGR}}\right) \tag{21}$$

When an under steered vehicle makes a circle of fixed radius and increases the speed from the stop, the steering wheel angle has to be increased with the speed. The speed when the steering angle is doubled is defined by Bosch as the characteristic speed, V_{ch}. The measured lateral acceleration is lead compensated using the acceleration calculated in equation (21) as the reference. The compensated lateral acceleration is upper limited by the acceleration given in equation (21) and again by the estimated load surface friction coefficient multiplied by g. Also, the measured signal is lower limited such that the compensated lateral acceleration always has the same sign as the steering input signal. Finally, the lead compensator is implemented with a first-order low pass filter to reject some high frequency noise. Figure 5 shows the example of the lead compensated lateral acceleration along with the measured lateral acceleration and the steering input. The initial vehicle speed is $100\,\text{km}\,\text{h}^{-1}$. The compensated signal leads the measured signal significantly and also rejects some parasitic high frequency oscillation.

The side slip angle information from the ESP algorithm is lead compensated in the similar way that the lateral acceleration is compensated using the preceding steering angle input signal. Unfortunately for the side slip angle, the steady state information derived from the bicycle model can be inaccurate due to the drifting of the signal. Knowing that more leading of the side slip angle is necessary for the higher vehicle speed and also for the more dynamic maneuver represented by the higher steering angle rate, the lead compensator is designed such that the lead term is proportional to the multiple of vehicle speed and steering rate. Then, the amplitude of the compensated signal is upper limited such that the magnitude does not exceed the maximum slip angle produced during the previous period of the maneuver. Finally, the compensated side slip angle is high pass filtered to eliminate the potential drifting of the angle. The drifting side slip angle can result in too much brake intervention for too long time period beyond the point of the rollover prevention. Figure 6 shows the example of the lead compensated side slip angle along with the estimated vehicle side slip angle from the ESP algorithm and the steering input. The initial vehicle speed is $100\,\text{km}\,\text{h}^{-1}$. The compensated signal precedes the raw input signal significantly.

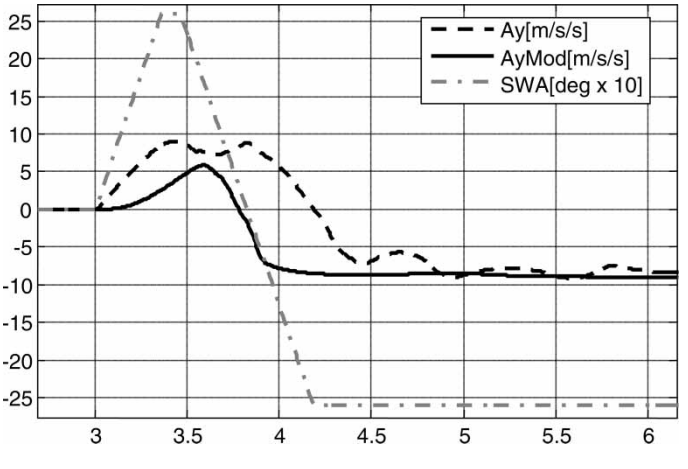

Figure 5. Example of lead compensated lateral acceleration.

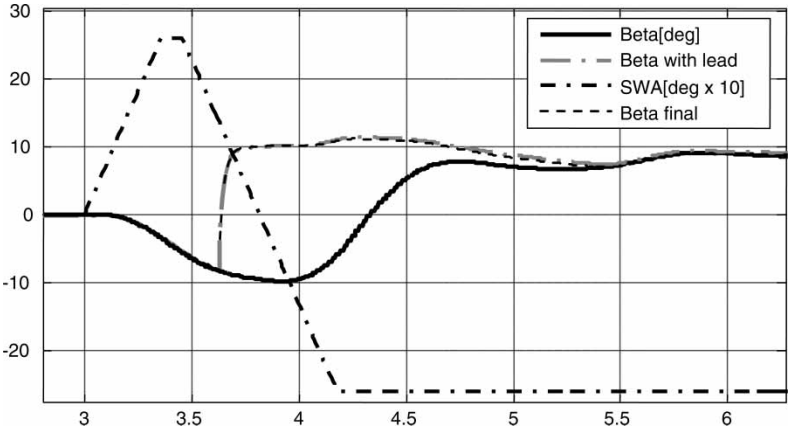

Figure 6. Example of lead compensated side slip angle.

5. Brake actuator sub-loop controller

The amount of the target wheel slip is defined to be proportional to the calculated ROI. The good performance of the actuator is important for the success of the wheel slip control, especially when the wheel slip target is at the deep unstable region of the μ-slip curve. In that region, the partial derivative of the tire-to-surface friction coefficient with respect to the wheel slip is negative. Therefore, it is very critical to remove the actuation delay to achieve a good slip control. In addition to the purpose of the good wheel slip control, it is equally important to remove any extra closed loop delay from the rollover prevention point of view. As mentioned before, vehicle rollover is a very dynamic process. Therefore, any slight delay of the actuation causes a huge increment of the control input that is not recommended for noise, vibration and harshness point of view. Unfortunately, the rollover avoidance controller has no choice but to use the existing actuator designed and optimized for the ESP – usually not fast enough for the purpose of the rollover avoidance control. Also, the production brake actuator used in this study suffers the poor resolution problem especially at a high pressure. The resolution is as large as 20 bars at 100 bar region especially for the dump cycle. Unfortunately, rollover avoidance control is operated at that pressure region most of the time. For the variation of

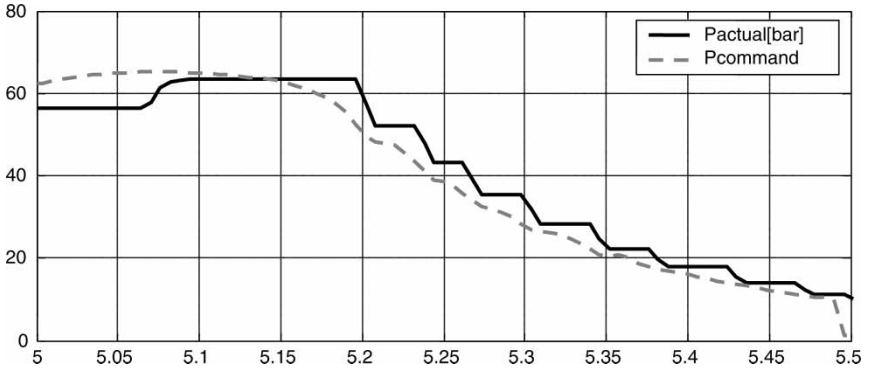

Figure 7. Original brake actuation without pressure control compensation.

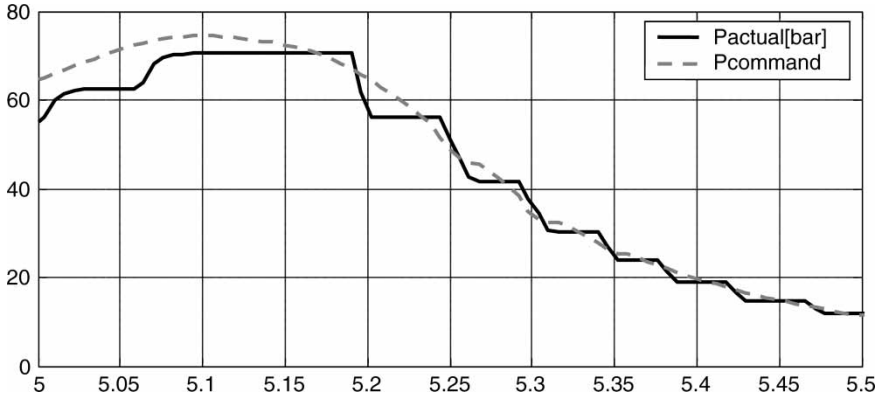

Figure 8. Brake actuation with proportional pressure control compensation.

the control command less than the resolution, the actuator does not respond, and that causes significant actuation delay as can be seen in figure 7.

The problem is fixed by implementing a simple proportional sub-loop controller described below:

$$\text{Pcmd2} = \text{Pcmd1} + \text{Pgain} * (\text{Pcmd1} - \text{Pestm}) \tag{22}$$

Where, Pcmd1 is the input of the sub-loop controller, Pcmd2 the output, Pgain the proportional gain and Pestm the estimated wheel pressure. The gain is set to be asymmetrical and the value is much larger for the negative error, considering the fact that dumping delay deteriorates the tracking performance of the unstable control system significantly. The effect of the sub-loop control is limited to $[-20, +20]$ bars since the worst case resolution is 20 bars. The following figure 8 shows the response of the pressure tracking after the actuator control is sub-loop compensated. The poor resolution problem remains, but the delay problem associated with it is resolved.

6. Control architecture

The architecture of the rollover prevention control system is as shown in figure 9. The ESP algorithm block reads steering wheel angle, yaw rate and lateral acceleration as well as wheel speeds and calculates vehicle side slip angle and longitudinal speed. The calculated side slip angle and the measured vehicle lateral acceleration are lead compensated in lead compensation block. Roll stability control block reads the lead compensated lateral acceleration and the side slip angle and calculated ROI. The accuracy of the calculated ROI can be enhanced with the adaptively observed C.G. height and the estimated roll angle information. They are the output of the optional roll angle observer block. The observer block needs the roll rate information of the vehicle in addition to ESP sensor signals. For the wheel control, pressure and wheel slip commands are defined. The commands are simply proportional to the calculated ROI. The commands are applied to the front outside wheel. The side is determined by the sign of the steering wheel angle. Similar pressure and wheel slip commands are also calculated from the ESP algorithm block. The duplicating wheel commands are arbitrated by the arbitrator algorithm block. Usually, the maximum of the commands – both for the pressure and the slip – are taken as the output of the arbitrator block. The wheel slip controller block reads the wheel pressure command and the wheel slip command. From the wheel slip command and the wheel slip tracking error, the wheel control pressure is calculated. The calculated control pressure is

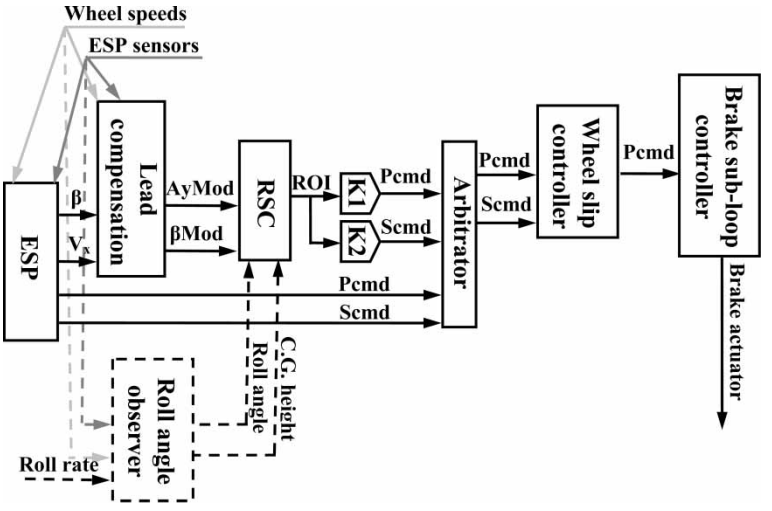

Figure 9. Diagram of control system architecture.

upper limited by the pressure command output from the arbitrator block. Finally, the pressure command from the slip controller block is compensated by the brake sub-loop controller block and sent to the brake actuator.

7. Test results

The performance of the developed rollover avoidance control algorithm is evaluated using a GM mid-size SUV. The ROI is defined without the roll rate sensor, i.e. without the roll kinetic energy. The vehicle is loaded with 100 kg of mass at the roof top. The forward velocity of the vehicle is just above 100 km h^{-1}. The test environment is a flat high μ surface.

Figure 10 shows the response of a fishhook type maneuver with very fast steering action from one side to other. The switching point of the steering wheel is determined to maximize the instability of the vehicle roll dynamics. During the first half of the steering maneuver (0–0.5 s), the rollover avoidance control is not activated. During the second half, both the rollover controller and ESP command the wheel brake controls. It should be noted that the rollover controller controls only the front wheels. The control commands are in similar shapes. However, the rollover control command precedes the ESP command by a few hundred milliseconds. During the rollover control, there is a deep slip of the controlled wheel speed, but the speed control is smooth and stable. The roll angle is not measured, but the roll dynamics is observed to be very smooth. Therefore, the measured lateral acceleration signal also remains very smooth. While preventing the rollover, it is equally important to prevent the over correction and to keep the vehicle still maneuverable. During the rollover control, the vehicle yaw rate is reduced significantly. However, the yaw rate keeps the same sign as the steering input and the vehicle stays maneuverable, e.g. the steering wheel is turned to the right-hand side, and the vehicle turns to the same side.

The significantly lead compensated rollover avoidance controller can suffer from the false brake actuation. However, any noticeable false activation of the brake pressure control is just not allowed. The developed rollover control algorithm needs to be evaluated thoroughly for the full spectrum of the vehicle tests representing the real life driving conditions. At one end of the spectrum is the fishhook type maneuver. It represents double lane change or obstacle

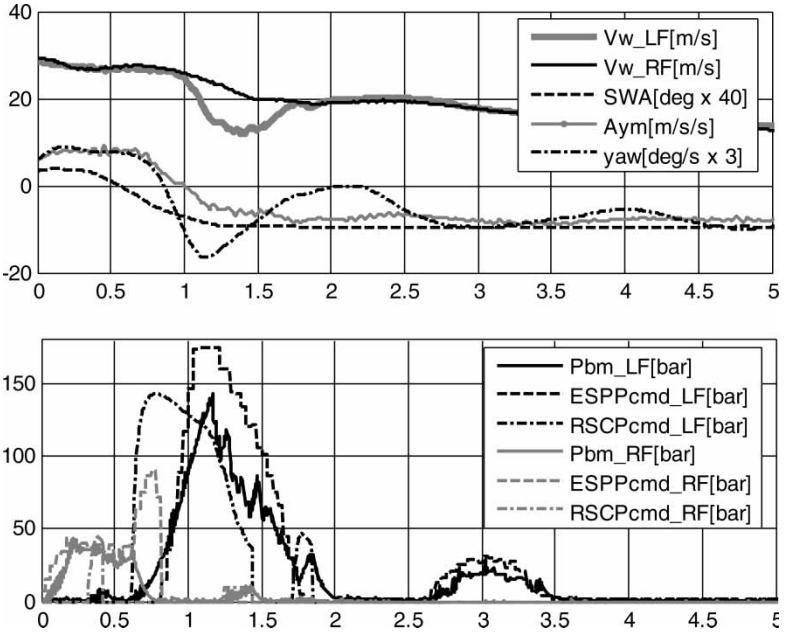

Figure 10. Fishhook type maneuver with fast steering action.

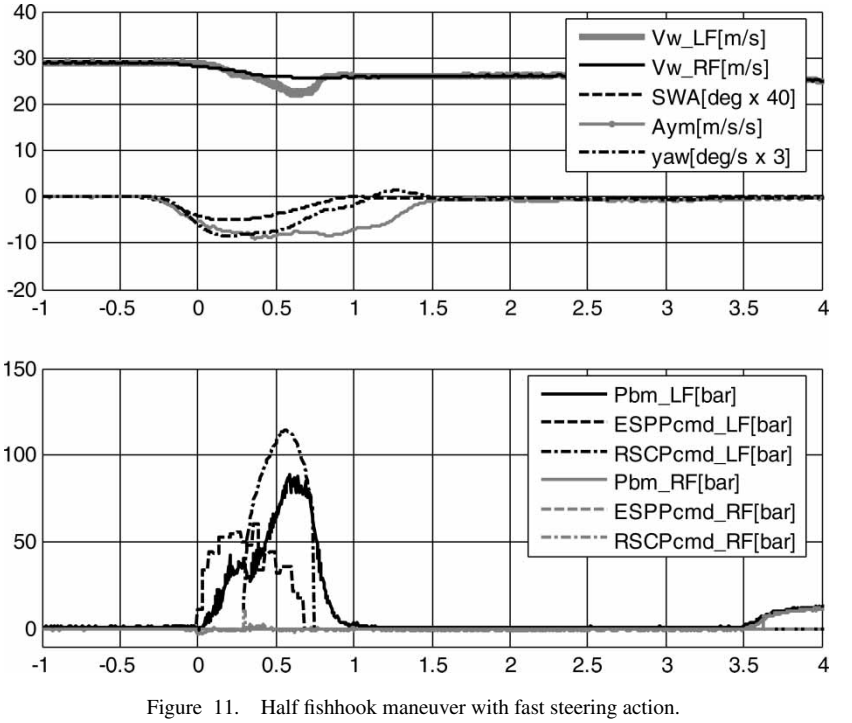

Figure 11. Half fishhook maneuver with fast steering action.

avoidance maneuver. Since it is the most severe dynamic maneuver with the most severe brake intervention, the sudden termination of the maneuver in the middle of it can cause the most severe false activation problem. To evaluate the severity and the frequency of the false activation, the half fishhook type maneuver is suggested. Figure 11 shows the typical steering

input during the half fishhook maneuver along with other measured signals and the control inputs. During the first half of the maneuver (0–0.8 s), ESP is activated lightly. While ESP is activated, the rollover control is activated very briefly. However, the rollover control command overlapping with the ESP wheel command is not large enough to be noticed by the driver. During the missing (zero steering angle) second half of the maneuver (after 0.9 s), the rollover control is not activated falsely at all.

8. Conclusions

A new concept of ROI has been developed from the lateral kinetic energy of a vehicle using only ESP sensor signals. Also, the rollover control algorithm has been developed to work with the existing production brake actuator that is somewhat slow for the purpose of the rollover control. The simulation results in several driving conditions show that the developed ROI represents the rollover propensitiy fairly accurately with enough lead time.

An adaptive observer has been designed to observe the roll angle and to update the vehicle C.G. height information. The stability and the performance of the developed adaptive observer have been proven by Lyapunov analysis and evaluated by computer simulation. The defined ROI can be further enhanced by including the calculated roll energy and updating the C.G. height information in real time adaptively.

The ESP signal lead compensators have been designed to cancel the lag effect of the brake actuation. The compensators lead the raw signals significantly without any side effects. A simple but very efficient brake sub-loop controller has been designed to further cancel the brake actuation lag effect.

The new concept of the rollover avoidance control has been implemented on a test vehicle. The test results show that the rollover prevention control is very robust for the fishhook type maneuvers with 100 kg of load on the roof top up to the speed of 110 km h^{-1} and beyond. Any noticeable false activation of the brake has not been observed. The controlled wheel pressure and the slip are very smooth, and therefore the ride quality is not harsh during the controls. Also, the vehicle stays maneuverable during the control.

Acknowledgements

The author thanks Arnie Spieker of TRW Automotive and Murali Gopinathan of Mathworks for their advice and help with the work of experimental validations.

References

[1] U.S. National highway traffic safety administration, report DOT HS-809–868.
[2] Matsumoto, S., Yamaguchi, H., Inoue, H. and Yasuno, Y., 1992, Improvement of vehicle dynamics through braking force distribution control, SAE Paper No. 920645, SAE Congress and exposition.
[3] Zanten, A. V., Erhardt, R. and Pfaff, G., 1995, VDC, the vehicle dynamics and control system of Bosch, SAE paper No. 950759, SAE Congress and exposition.
[4] Lee, A. Y., 2002, Coordinated control of steering and anti-roll bars to alter vehicle rollover tendencies. *ASME Journal of Dynamic Systems, Measurement and Control*, **124**, 127–132.
[5] Gaspar, P., Szaszi, I. and Bokor, J., 2003, Rollover avoidance for steer-by-wire vehicles by using linear parameter varying methods. Proceedings of Mediterranean Conference on Control and Automation, Rhodes, Greece.
[6] Odenthal, D., Bunte, T. and Ackermann, J., 1999, Nonlinear steering and braking control for vehicle rollover avoidance. Proceedings of European Control Conference, Karlsruhe, Germany.
[7] Hac, A., 2002, Influence of active chassis systems on vehicle propensity to maneuver-induced rollovers, *SAE* Paper No. 2002-01-0967, SAE Congress and exposition, Detroit, USA.
[8] Ackermann, J., Bnte, T., Odenthal, D. and Bunte, T., 1999, Advantages of active steering for vehicle dynamics control, Proceedings of International Symposium on Automotive Technology and Automation, Vienna.

[9] Garrick, J. F., Garrott, W. K. and O'Harra, B.C., 2002, A comprehensive experimental examination of test maneuvers that may induce on-road untripped light vehicle rollover – Phase IV, NHTSA Light vehicle rollover research program, DOT HS 809 513.
[10] National highway traffic safety administration, 2002, Traffic safety facts 2001.
[11] Nalecz, A.G. and Bindemann, A.C., 1987, Sensitivity analysis of vehicle design attributes that affect vehicle response in critical accident situations – part I: user's manual, DOT-HS-807-229, U.S. Department of Transportation, National Highway Transportation Safety Administration.
[12] Yamaguchi, H., Asano, K., Yasui, Y. and Ito, T., 1997, The estimation method of side slip angle. *JSAE Review*, **18**(2), 190.
[13] Chumsamutr, R., Fujioka, T. and Abe, M., 2006, Sensitivity analysis of side-slip angle observer based on a tire model. *Vehicle System Dynamics*, **44**(7), 513–527.
[14] Sasaki, H., 2000, A side-slip angle estimation using neural network for a wheeled vehicle, SAE 2000-01-0695.
[15] Hiraoka, T., Kumamoto, H. and Nishihara, O., 2004, Sideslip angle estimation and active front steering system based on lateral acceleration data at centers of percussion with respect to front/rear wheels, *JSAE Review*, **1**, 37–42.
[16] Hac, A. and Simpson, M., 2000, Estimation of vehicle side slip angle and yaw rate, SAE 2000-01-0696.
[17] Fukada, Y., 1999, Slip-angle estimation for vehicle stability control. *Vehicle System Dynamics*, **32**(4–5), 375–388.
[18] Krantz, W., 2002, Estimation of side slip angle using measured tire forces, SAE 2002-01-0969.
[19] Germann, S. and Isermann, R., 1994, Determination of the centre of gravity height of a vehicle with parameter estimation. IFAC Symposium on system identification, Copenhagen.
[20] Ackermann, J. and Odenthal, D., 1998, Robust steering control for active rollover avoidance of vehicles with elevated centre of gravity. Proceedings of International conference on advances in vehicle control and safety, Amiens, France.
[21] Rajamani, R., 2005, *Vehicle Dynamics and Control* (New York: Springer Inc).